2018 European Control Conference (ECC)
June 12-15, 2018. Limassol, Cyprus

Stability Verification for Periodic Trajectories of Autonomous Kite Power Systems

Eva Ahbe, Tony A. Wood, Roy S. Smith

Abstract— **State-feedback controllers are frequently employed in Airborne Wind Energy systems to follow reference flight paths. In this paper we compute the region of attraction (ROA) of path-stabilizing feedback gains around a periodic trajectory as typically flown by a power generating kite. The feedback gains are obtained from applying a time-varying periodic Linear Quadratic Regulator to the system expressed in transversal coordinates. To compute the ROA we formulate Lyapunov stability conditions which we verify by Sum-of-Squares programs. These programs are posed as an optimization problem for which we compare various definitions of the cost function representing the size of the ROA. In a numeric case study we demonstrate that the maximization of an expanding ellipse inside of quartic Lyapunov functions leads to significantly larger verified ROAs compared to the standard approach of optimizing over the scaling of the sublevel set of a quadratic Lyapunov function.**

I. Introduction

Autonomous power kites are an emerging technology in the field of Airborne Wind Energy (AWE) systems, which aim at exploiting the strong and consistent winds found at higher altitudes than currently accessible by conventional horizontal-axis wind turbines. The concept of generating power by exploiting large forces acting on kites flying in crosswind conditions was originally introduced in [1]. Since then several different prototype systems have been suggested and implemented. An overview of the technology can be found in [2].

In the attempt to provide full autonomous operation, a wide variety of control approaches have emerged. While many approaches have lead to successful autonomous flight experiments [3]–[6], the issue of reliability, i.e. having guarantees for the desired behavior of the kite, is still an open problem. A common approach for achieving desired flight behavior is the regulation of the deviation of the kite position from a reference path [5], [7], [8]. Formally, a way of providing reliability is given by guaranteeing the stabilizing impact of the feedback controller on the kite path deviation. Thereby, the stabilizing impact can be quantified by assessing the region of attraction (ROA) of the feedback stabilized system.

In previous work [9]–[12], the ROA of path-following feedback controllers along reference trajectories was verified via semidefinite programming. We follow this approach here and present a path-following method, based on a kinematic kite motion model, for which we compute the region in which the controller is guaranteed to stabilize the path deviation from a power-optimal, periodic, figure-of-eight trajectory. This trajectory represents a limit cycle of the closed-loop system for which we obtain stabilizing feedback gains from a time-varying periodic Linear Quadratic Regulator (LQR).

Due to the periodic nature of our problem we follow the procedure of obtaining ROA estimates which is tailored to limit cycles and presented in [11]–[13]. Therein, the system is transformed into transversal coordinates such that the ROA can be verified through a Lyapunov stability analysis. The resulting conditions for stability are tested via sum-of-squares (SOS) programs that result from a semidefinite relaxations of the stability condition, as proposed in [14]. The tested conditions are thereby sufficient, thus allowing for optimization algorithms which test for larger verified ROAs. The standard approach in optimizing the verified ROA of limit cycles consists of time-varying scalings of the sublevel sets of time-varying quadratic Lyapunov functions (LF) [11]–[13]. In previous work on the ROA of equilibrium points of nonlinear systems [15], [16], a common approach consisted of expanding an ellipse of fixed shape inside LF sublevel sets in order to estimate the ROA. We extend this approach, firstly, by applying it to the ROA analysis of limit cycles and, secondly, by expanding an ellipse of variable shape instead of a fixed one inside of LF sublevel sets. With this extension we are also able to maximize over higher order LFs than the quadratic ones commonly used for limit cycles. By applying these different approaches in our numeric case study we show how with the extended approach we were able to verify larger ROAs compared to the standard approaches.

A. Notation

We use ∂ to denote the degree of a polynomial. We use $\mathbb{R}[x]$ for the ring of polynomials with real coefficients in the indeterminants $[x_1, ..., x_n]$. A polynomial is SOS if it can be written as $p(x) = \sum_i q_i^2$, $q_i \in \mathbb{R}[x]$. The set of all SOS polynomials is indicated by $\Sigma[x]$. If $p(x)$ is SOS then $p(x) \geq 0$ for all x and we can find a matrix $Q \succeq 0$ s. t. $p(x) = z(x)^T Q z(x)$, where $z(x)$ is the vector of monomials up to degree $\partial/2$. For $\omega \in \mathbb{R}$ and a polynomial $g : \mathbb{R}^n \to \mathbb{R}$, the ω-sublevel set $\Omega_{g,\omega}$ is defined as $\Omega_{g,\omega} := \{x \in \mathbb{R}^n \mid g(x) \leq \omega\}$. We define the distance of a point $x \in \mathbb{R}^n$ to a set $K \subset \mathbb{R}^n$ by $\text{dist}(x, K) := \min_{y \in K} ||x - y||_2$.

*This work was supported by the Innovative Training Network (ITN) project funded by the European Union's Horizon 2020 research and innovation programme under the Marie Sklodowska-Curie Action (MSCA), grant agreement No. 642682.

The authors are with the Automatic Control Laboratory, Swiss Federal Institute of Technology (ETH Zurich), Physikstrasse 3, 8092 Zurich, Switzerland, {ahbee,woodt,rsmith}@control.ee.ethz.ch

II. Model and Trajectory Generation

In this section we set up the problem of controlling the deviation of a kite from a desired flight path by introducing first the model of the kite system and then the algorithm for generating the desired reference trajectory.

A. Kite Model

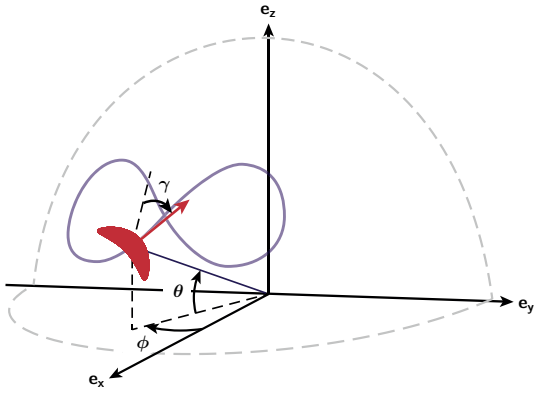

Fig. 1. Illustration of coordinate system. θ denotes the elevation angle, ϕ the azimuth angle and γ the orientation angle of the kite where $\gamma = 0$ when the kite is pointing towards the zenith.

We represent the dynamics of the kite by a first order kinematic model of the states $x = (\theta, \phi, \gamma)$, where θ denotes the elevation angle, ϕ denotes the azimuth angle, and γ denotes the orientation angle of the kite (see Figure 1),

$$\dot{\theta} = \frac{v_k}{L}\cos(\gamma), \tag{1a}$$

$$\dot{\phi} = \frac{v_k}{L}\cos(\theta)^{-1}\sin(\gamma), \tag{1b}$$

$$\dot{\gamma} = v_k G_s u, \tag{1c}$$

$$v_k = v_w E\,\cos(\theta)\,\cos(\phi), \tag{1d}$$

where $E = C_L/C_D$ is the glide ratio with C_L being the lift coefficient and C_D the drag coefficient. L is the line length, v_w is the wind speed, and G_s is the steering gain. All these parameters are assumed to be constant. The input u is proportional to the rate of change of the orientation of the kite. This kinematic model is similar to the models employed for guidance control design in [4], [8].

B. Trajectory Generation

In order to generate power-optimal periodic reference trajectories for the model in (1), we use the optimal control software GPOPS-II [17]. The optimization problem we solve is stated as follows:

$$\max_{x(\cdot),u(\cdot),x_0,T_f} \quad \frac{1}{T_f}\int_0^{T_f} F(x(t),u(t))dt \tag{2}$$

subject to:

$\forall t \in [0,T]$:

$$\dot{x} = f(x(t),u(t))$$
$$\underline{c} \le x(t) \le \overline{c}$$
$$\underline{b} \le u(t) \le \overline{b}$$
$$x(0) = x(T) = x_0$$

where $F(x(t),u(t))$ is the force exerted by the kite on the tether resulting from an equilibrium of the aerodynamic forces (see e.g. [1]). The function $f(x(t),u(t))$ represents the dynamics in (1), $(\underline{c}, \overline{c}) \in \mathbb{R}^3$ denote the state constraints and $(\underline{b}, \overline{b}) \in \mathbb{R}$ are the upper and lower input constraints. The constraints are chosen such that the trajectory lies in crosswind flight condition, a minimum altitude is maintained for safety and the input respects the physical limitations of the kite, such as maximum turning rate. Further, we add a periodicity constraint to obtain a closed orbit $\Gamma^* = \{(x^*(t),u^*(t)) \,|\, t \in [0,T)\}$ as the optimal reference trajectory.

III. Stability of Orbits

In this section we will introduce the notion of orbital stability and the transformation to transversal coordinates which will later allow us to analyse the stability of the closed loop system when following the reference trajectory.

A. Orbital Stability Definition

The definitions stated here are standard (see, e.g., [18], [19]). The solution of an autonomous dynamical system, such as closed-loop systems,

$$\dot{x} = h(x), \tag{3}$$

with state $x(t) \in \mathbb{R}^n$ and $x(0) = x_0$, is denoted by $\phi(x_0,t)$ for $t > 0$.

A periodic orbit is defined by a solution $\tilde{x}(t) = \phi(\tilde{x}_0,t)$ which satisfies $\tilde{x}(0) = \tilde{x}(T)$ with the period being the minimum $T > 0$. The periodic orbit Γ is denoted by

$$\Gamma = \{x \in \mathbb{R}^n | x = \tilde{x}(t),\, t \in [0,T]\}. \tag{4}$$

The periodic orbit (4) is called asymptotically (orbitally) stable if it is stable, i.e. $\forall \epsilon > 0, \exists \delta > 0$ such that $\forall x_0 \in \mathbb{R}^n$ with $\text{dist}(x_0,\Gamma) < \delta$ we have $\text{dist}(\phi(x_0,t),\Gamma) < \epsilon$, $\forall t > 0$, and if it is attractive, i.e. $\exists \delta > 0$ such that $\forall x_0 \in \mathbb{R}^n$ with $\text{dist}(x_0,\Gamma) < \delta$ we have $\lim_{t\to\infty} \text{dist}(\phi(x_0,t),\Gamma) = 0$.

A set $K \subset \mathbb{R}^n$ with $\text{int}(K) \neq \emptyset$ and $\Gamma \subset \text{int}(K)$ is called an inner estimate of the region of orbital stability of $\tilde{x}(\cdot)$ if $\forall x_0 \in K$ we have $\text{dist}(\phi(x_0,t),\Gamma) \to 0$ as $t \to \infty$.

The aim of this paper is to obtain inner estimates of the region of attraction for a periodic solution of the feedback stabilized kite dynamics (1). In [19] it is shown that a periodic orbit is exponentially stable if and only if the linearization of the system in transversal coordinates is asymptotically stable. Since asymptotic stability of linearizations can efficiently be investigated with Lyapunov's Method (see e.g. [20]), we apply a coordinate transformation into transversal coordinates.

B. Transversal Coordinates

Transversal coordinates were defined both in [21] and in [19] and were applied in [11], [12] and [13] for the stability analysis of hybrid systems with limit cycles. Here, we employ the transformation laws as derived in full detail in [21] and [11]. Transversal coordinates are obtained from a smooth and locally well-defined transformation of any $x \in \mathbb{R}^n$ in a sufficiently close neighborhood of the orbit Γ

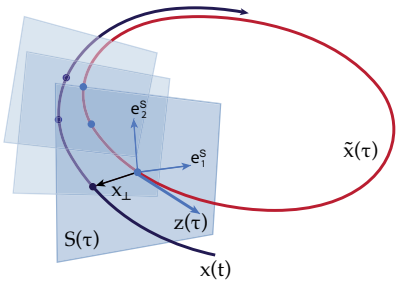

Fig. 2. Illustration of the transversal coordinates used to analyse orbital stability. The hyperplanes $S(\tau)$ are defined by a $(n-1)$-dimensional coordinate system e_i^S, $i = 1, ..., n-1$. The vector $\mathrm{z}(\tau)$ is normal to the hyperplane $S(\tau)$.

into a set of coordinates $(\tau, x_\perp) \in S^1 \times \mathbb{R}^{n-1}$. For every $t \in [0, T)$ we can then define a $(n-1)$-dimensional time-varying hyperplane S with $S(0) = S(T)$, which is transversal to Γ at $\tilde{x}(t)$. Given any x in a sufficiently close neighborhood of $\tilde{x}$, τ specifies the corresponding transversal hyperplane and $x_\perp$ is the position on that hyperplane. From this definition it follows that $x_\perp = 0 \Leftrightarrow x = \tilde{x}(\tau)$. For a visualization see Figure 2. The transversal hyperplanes $S(\tau)$ are defined as

$$S(\tau) = \{x \in \mathbb{R}^n | z(\tau)^T (x - \tilde{x}(\tau)) = 0\},$$

where $z(\tau) : [0, T) \to \mathbb{R}^n$ is a smooth, periodic vector function that is to be chosen. We require $z(\tau)$ to satisfy

$$z(\tau)^T f(\tilde{x}(\tau), \tilde{u}(\tau)) > 0, \tag{5}$$

for all $\tau \in [0, T)$.

A common choice of $z(\tau)$, which we use here, consists of defining the transversal hyperplanes orthogonal to the system motion (as e.g. in [21]), i.e. $z(\tau) = \frac{f(\tilde{x}(\tau), \tilde{u}(\tau))}{||f(\tilde{x}(\tau), \tilde{u}(\tau))||_2}$.

As such, z is tangential to the motion of the system and is normalized for numerical simplicity. Even though [11] and [13] have shown that this choice of z can impose limitations that later lead to conservative estimates of the ROA, we have found that for our problem it is not the limiting factor and thus is a suitable choice.

With this choice of z we can construct a projection operator as described in [21] that maps any point x in the neighborhood of Γ into its transversal coordinates on the corresponding hyperplane

$$x_\perp = \Pi(\tau)\,(x - \tilde{x}(\tau)). \tag{6}$$

We can then state the dynamics of the system in transversal coordinates (for derivations see [11]) as

$$\begin{aligned}\dot{x}_\perp = &\left[\frac{d}{d\tau}\Pi(\tau)\right]\dot{\tau}\Pi(\tau)^T x_\perp \\ &+ \Pi(\tau) f(\tilde{x}(\tau) + \Pi(\tau)^T x_\perp, u(x_\perp, \tau)),\end{aligned} \tag{7}$$

$$\dot{\tau} = \frac{z^T f(\tilde{x}(\tau) + \Pi(\tau)^T x_\perp, u(x_\perp, \tau))}{z(\tau)^T f(\tilde{x}(\tau), u(x_\perp, \tau)) - \frac{\partial z(\tau)}{\partial \tau}^T \Pi(\tau)^T x_\perp}, \tag{8}$$

where the state-feedback policy $u(x_\perp, \tau)$ is left to be designed. In order for the dynamics of τ to be well-defined, the denominator of (8) must not be zero. From condition (5), we additionally know that the first term in the denominator is positive. Since the second term is a linear function of $x_\perp$ for a fixed τ, we obtain as a condition for the transformation to transversal coordinates to be well-defined,

$$z(\tau)^T f(\tilde{x}(\tau), \tilde{u}(\tau)) - \frac{\partial z(\tau)}{\partial \tau}^T \Pi(\tau)^T x_\perp > 0. \tag{9}$$

C. Transverse Linearization

Since in this work we consider a state-feedback stabilized kite system (1) for path-following, we state in the following the transverse linearization required for state feedback control of a system in transversal coordinates. In general, we have several options for feedback controller design, such as the LQR or $\mathcal{H}_\infty$-based methods. Assuming transversal surfaces orthogonal to the system motion, the linearization of the transverse dynamics (7), (8) is

$$\dot{x}_\perp = A_\perp(\tau) x_\perp + B_\perp(\tau) u_\perp, \tag{10}$$

where $u_\perp = u - \tilde{u}(\tau)$ is the transverse component of the input resulting from the feedback control, and $A_\perp(\tau), B_\perp(\tau)$ are obtained from linearizing (7) around $\tilde{x}, \tilde{u}$ (i.e., $x_\perp = 0$)

$$\begin{aligned}A_\perp(\tau) = &\left[\frac{d}{dt}\Pi(\tau)\right]\Pi(\tau)^T \\ &+ \Pi(\tau)\frac{\partial f(\tilde{x}(\tau), \tilde{u}(\tau))}{\partial x}\Pi(\tau)^T,\end{aligned} \tag{11}$$

$$B_\perp(\tau) = \Pi(\tau)\frac{\partial f(\tilde{x}(\tau), \tilde{u}(\tau))}{\partial u}. \tag{12}$$

The state feedback stabilized system can then be regarded as an autonomous system (3).

IV. Region of Attraction Verification

In this section we state the stability conditions we need to test in order to obtain an inner approximation of the ROA of an autonomous system (3). For closed-loop systems, the ROA obtained from this analysis represents the region in which the feedback gains stabilize the system. The stability conditions are sufficient conditions and can be formulated as semidefinite programs (SDPs). In order to test for larger inner approximations we explore different cost functions in the SDPs which serve as surrogates for the size of the ROA.

A. Lyapunov Stability Conditions

The stabilizing gains obtained from a feedback controller applied to a system $f(x_\perp, u_\perp)$ are computed for the transverse linearization of the dynamics. From Lyapunov's Indirect Method (see, e.g., [20]), we know that these feedback gains will also stabilize the nonlinear system in some neighborhood of the reference trajectory $\tilde{x}(\cdot)$. This neighborhood, the ROA, can be found using the following theorem:

Theorem (Theorem 2, from [11]) Suppose there exists a function $V : \mathbb{R}^{n-1} \times \mathbb{R} \to \mathbb{R}$ such that $\Omega_{V,1} := \{(x_\perp, \tau) \mid V(x_\perp, \tau) \leq 1\}$ is compact and for which the

following inequalities hold for all $(x_\perp, \tau) \in \Omega_{V,1}$

$$V(x_\perp, \tau) > 0, \quad x_\perp \neq 0, \quad (13)$$

$$\dot{V}(x_\perp, \tau) < 0, \quad x_\perp \neq 0, \quad (14)$$

$$V(0, \tau) = \dot{V}(0, \tau) = 0, \quad (15)$$

$$d(x_\perp, \tau) := z(\tau)^T h(\tilde{x}(\tau)) - \frac{\partial z(\tau)}{\partial \tau}^T \Pi(\tau)^T x_\perp > 0, \quad (16)$$

then $\Omega_{V,1}$ is an inner estimate for the region of orbital stability of $\tilde{x}(\cdot)$.

With $\dot{\tau} = \frac{n(x_\perp, \tau)}{d(x_\perp, \tau)}$ and dropping the $(x_\perp, \tau)$-notation,

$$\dot{V} = \frac{\partial V}{\partial x_\perp} \left[\left[\frac{d\Pi}{d\tau} \right] \Pi^T x_\perp n + \Pi h(\tilde{x} + \Pi^T x_\perp) d \right] + \frac{\partial V}{\partial \tau} n. \quad (17)$$

where we removed $d(x_\perp, \tau)$ from the denominator by multiplying $\dot{V}$ with it. This does not change the result from condition (14) as $d(x_\perp, \tau)$ is constrained to be positive. Our aim in the following is to maximize the region of orbital stability, i.e. the ROA, given by the $\Omega_{V,1}$ for which stability is verified by the Theorem above. For a polynomial system, finding $\Omega_{V,1}$ can be reduced to a question of set emptiness, expressed by a finite number of polynomial equalities and inequalities. In general, these are NP-hard problems to solve. In [14] a formulation was introduced to relax this class of semialgebraic problems into SDPs using SOS polynomials. This is done by employing Stengle's Positivstellensatz [22].

B. Verification via SOS-Programs

In order to use semidefinite relaxations to verify the stability region $\Omega_{V,1}$, we need the transverse dynamics (7),(8) of the kite system to enter in the conditions (14)-(16) in polynomial form. We therefore approximate the dynamics (1) by a Taylor series up to third order.

We can formulate the SDP resulting from the relaxation such that we not only test the conditions (13)-(16) for feasibility but at the same time also maximize the inner estimate of the ROA. The corresponding optimization problem is

$$\max_{V, s_1, s_2} \quad \text{volume}(\Omega_{V,1}) \quad (18a)$$

$$\text{subject to} \quad V(x_\perp, \tau) - l(x_\perp) \in \Sigma[x_\perp, \tau] \quad (18b)$$

$$-\dot{V}(x_\perp, \tau) - (1 - V(x_\perp, \tau)) s_1(x_\perp, \tau) - l(x_\perp) \in \Sigma[x_\perp, \tau] \quad (18c)$$

$$d(x_\perp, \tau) - (1 - V(x_\perp, \tau)) s_2(x_\perp, \tau) \in \Sigma[x_\perp, \tau] \quad (18d)$$

$$s_1(x_\perp, \tau), s_2(x_\perp, \tau) \in \Sigma[x_\perp, \tau] \quad (18e)$$

The LF $V(x_\perp, \tau)$ is polynomial in both $x_\perp$ and τ. The polynomial $l(x_\perp)$ is fixed and positive. It results from the condition $x_\perp \neq 0$ for both $V(x_\perp, \tau) > 0$ and $\dot{V}(x_\perp, \tau) < 0$ in the implementation of the Positivstellensatz, and is here chosen as $l = \epsilon ||x_\perp||_2^2$ where ϵ is small fixed positive constant. The polynomials s_1 and s_2 are SOS-multipliers whose maximum degree is to be chosen by the user. Other than the restriction of being SOS, the multiplier polynomials can be chosen arbitrarily. The semidefinite relaxations of the Positivstellensatz which are represented by the constraints in (18) provide sufficient conditions for stability defined as in the Theorem in Section IV-A. If the problem is not feasible for a chosen degree of multipliers it might still be feasible for higher degrees. The latter have the potential to verify larger regions, however computational costs increase significantly.

The optimization problem (18) is bilinear in the variables V and s_1, s_2. As done in previous work by [15],[10] and others, we approach the optimization by alternatingly fixing V while performing the optimization over s_1 and s_2, and, then fixing s_1 and s_2 while optimizing over V. Both steps of the optimization problem can then be solved efficiently as SDPs. The alternation can be initialized by using an initial candidate LF obtained from the solution $P(\tau)$ of the periodic differential Lyapunov equation [19] for the the transverse linearization of (3): $V_{\text{ini}}(x_\perp, \tau) = x_\perp^T P(\tau) x_\perp$.

If the chosen feedback controller is an LQR an initial LF can be obtained from the optimal cost resulting from the solution of the Riccati equation, as proposed in [9].

Since the constraints in (18) consider the 1-sublevel set of the LF we have to scale the initial candidate before starting the optimization via a bisection until the first iteration is feasible. We then iterate through the two optimization steps until we reach convergence of the verified region.

The optimization (18) is continuous both in $x_\perp$ and in τ. In order to make the problem computationally efficient we follow the approach in [10], [23] and discretize τ to then perform the optimization over the set of N fixed τ-values. This effectively chooses fixed transversal hyperplanes, equally spaced around the trajectory, and verifies the ROA on those chosen hyperplanes (see Figure 2). We denote the in τ-discretized polynomials with a superscript i in the following.

The objective function in the optimization problem (18) needs to be both convex as well as providing a comparable measure for the inner estimate of the ROA. We have several options depending on the complexity of LFs we want to optimize over and on how we measure the size of the verified sublevel set. We evaluate the different choices as follows, ordered with increasing complexity.

Scaling sublevel set of fixed V (SSS-fix$V$): Here we take the initial LF $V_{\text{ini}}^i = V_0^i$ fixed for all iterations of the optimization. We define $V^i = \frac{V_0^i}{\rho}$ and optimize $\Omega_{V_0^i, \rho}$ by maximizing the sublevel set ρ. The constraints (18b) - (18d) then contain, in discretized form, the term $(\rho - V_0^i)$ instead of the term $(1 - V^i)$.

Scaling sublevel set of quadratic V (SSS-$\partial(2)V$): In addition to the constant parametrization by ρ we parametrize V_0^i as a function which is continuous in both $x_\perp$ and τ, piece-wise linear (PWL) in τ and quadratic in $x_\perp$. We use the approximation

$$\frac{\partial V_0^i(x_\perp)}{\partial \tau} \approx \frac{V_0^{i+1}(x_\perp) - V_0^i(x_\perp)}{\tau^{i+1} - \tau^i}, \quad i = 1, ..., N\text{–}1, \quad (19)$$

in (17), similar to, e.g., [23]. To prevent the optimization increasing ρ by solely rescaling the PWL parametrization of V_0, we have to additionally impose a scaling constraint in the optimization over V_0^i, e.g. by $V_0^i(\sum_j e_j^{S_i}) = V_{\text{ini}}^i(\sum_j e_j^{S_i})$ as in [23]. Here, the $e_j^{S_i}$ denote the unit vectors of S^i.

Scaling ellipse inside variable-degree-V sublevel set (SESS-$\partial(m)V$): Higher degree LFs have the potential to enlarge the verified ROA. However, a way to measure the ROA is needed in order to efficiently optimize for the inner estimate. We employ a method similar to the approach used for ROA estimates of equilibrium points by [15], [16]. Here, the optimization enlarges a quadratic geometric figure of analytically computable volume inside the LF sublevel sets

$$b(x_\perp) = x_\perp^T B x_\perp, \;\; B \in R^{(n-1)\times(n-1)}, \;\; B \succ 0. \qquad (20)$$

As in [15], [16], the ellipse parameter B is taken as fixed B_0 such that the ellipse is given as $b_0(x_\perp) = x_\perp^T B_0 x_\perp$. This results in the set constraint

$$\Omega_{b_0,\beta} = \{x_\perp \in \mathbb{R}^{n-1} \,|\, b_0(x_\perp) \leq \beta\}, \quad \Omega_{b_0,\beta} \subset \Omega_{V^i,1}.$$

The volume is then maximized by optimizing over β. Now, LFs of any (even) degree m can be searched over in the optimization.

Expanding ellipse inside variable-degree-V sublevel set (EE-$\partial(m)V$): We extend the SESS-$\partial(m)V$ approach by, instead of a fixed B_0, using a variable B in the optimization, thus maximizing the volume of the ellipse both in shape and scaling. This results in the set constraint

$$\Omega_{b,1} = \{x_\perp \in \mathbb{R}^{n-1} \,|\, b(x_\perp) \leq 1\}, \quad \Omega_{b,1} \subset \Omega_{V^i,1}. \qquad (21)$$

We maximize (20) by minimizing the geometric mean of the eigenvalues of B, which is a convex problem. Note, that we need a sufficiently small $b(x_\perp)$ for the initialization of the optimization, which we can obtain from the smallest candidate LF sublevel set. Again, the LFs we then search over in the optimization can be of any degree and we define them to be piecewise linearly parametrized in τ as in (19). However, in this case the sublevel set is fixed to one such that an additional normalization constraint is not needed.

Using the EE-$\partial(m)V$ method and dropping the variable dependence notation, the two-step optimization is

Step 1: Finding multipliers

$$\max_{s_1^i, s_2^i, s_3^i, \xi^i, \forall i \in [1,N]} \quad \xi^i \qquad (22a)$$

$$\text{subject to} \quad -\dot{V}^i - (1 - V^i)s_1^i - l - \xi^i_{(1)} \in \Sigma[x_\perp] \qquad (22b)$$

$$d^i - (1 - V^i)s_2^i - \xi^i_{(2)} \in \Sigma[x_\perp] \qquad (22c)$$

$$-(1-b)s_3^i + (1 - V^i) - l - \xi^i_{(3)} \in \Sigma[x_\perp] \qquad (22d)$$

$$s_1^i, s_2^i, s_3^i \in \Sigma[x_\perp]$$

Step 2: Expanding ellipse

$$\max_{B, V^i, \forall i \in [1,N]} \quad -\det(B)^{1/n} \qquad (23a)$$

$$\text{subject to} \quad V^i - l \in \Sigma[x_\perp] \qquad (23b)$$

$$-\dot{V}^i - (1 - V^i)s_1^i - l \in \Sigma[x_\perp] \qquad (23c)$$

$$d^i - (1 - V^i)s_2^i \in \Sigma[x_\perp] \qquad (23d)$$

$$-(1-b)s_3^i + (1 - V^i) - l \in \Sigma[x_\perp] \qquad (23e)$$

where the additional constraints (22d) and (23e) ensure that the expanding ellipse (20) is fully contained in $\Omega_{V^i,1}$ as stated in (21). In (22) we maximize the components of the slack variable $\xi^i \in \mathbb{R}^3, i = 0, .., N$. We obtain a feasible solution for the stability conditions in the first step (22) when a positive ξ^i is returned.

In the following we summarize some of the technical details of our implementation.

a) The degree of the lowest term in the LFs is fixed to 2 since we require V to be SOS and zero for $x_\perp = 0$.
b) The degree of the multipliers are set to $\partial(s_1) = 4$, $\partial(s_2) = 2$, $\partial(s_3) = 2$. Additionally, we drop the constant and linear terms in s_1 for numerical reasons.
c) The first step (22) is a feasibility test and the use of a slack variable is optional. However, maximizing a slack in the first step can significantly decreases the number of iterations required until convergence.

V. Results

We generate an optimal figure-of-eight trajectory by solving (2). We thereby set the state constraints for θ and ϕ to correspond to the wind window, e.g. the quarter sphere defined by the y-axis and the positive parts of the x- and z-axes. The state γ is constrained to $[-\pi, +\pi]$ in order to force the kite to fly the figure-of-eight in upwards direction at the outer borders and prevent it from looping. The input constraints are chosen such that physical limits of the kite's turning rate are accounted for. We then stabilize the path-deviation of the kite system with feedback gains obtained from the periodic formulation of the time-varying LQR as found in [24]. Having chosen γ as state variable and its scaled derivative as input enables us to explicitly penalize the rate of change of γ in the LQR tuning and thus avoid overly aggressive changes of the input in the feedback design. We did not impose further input constraints which, however, could be additionally included at this point, if needed. The resulting optimal trajectory has a period of $T = 2.43s$.

The verification algorithm is implemented using the SOS-module of YALMIP [25] and MOSEK version 8.0 for solving the semidefinite programs. In our computations we discretized τ by $N = 100$, thus computing the ROA of the limit cycle in transversal coordinates on 100 hyperplanes equally spaced around the nominal trajectory. Figures 3 and 4 show the ROA resulting from the optimization in which the EE-$\partial(4)V$ method was used. The ROA is interpolated in between the slices for illustration purposes.

Figure 5 compares the size of the inner estimates of the ROA using the different methods with various LF degrees, i.e. SSS-fix$V$, SSS-$\partial(2)V$, SESS-$\partial(2)V$, SESS-$\partial(4)V$, EE-$\partial(2)V$ and EE-$\partial(4)V$. Since the verification algorithm can only test sufficient conditions, we used the same degree for the multipliers for all cases in order to obtain a fair comparison. The size of the inner estimates of the ROA displayed in Figure 5 were computed numerically by fitting a 100-sided polygon into the verified LF sublevel set and then computing the area of the polygon.

We find that the EE-$\partial(m)V$ method gives the largest lower bounds of ROA for both $\partial(2)$-V and $\partial(4)$-V. For both SESS-$\partial(m)V$ and EE-$\partial(m)V$, the $\partial(4)$-LF resulted in

larger estimates compared to the results from the quadratic V. Here, we also find that even though the run time per iteration was significantly longer due to the increased computational cost, the number of iterations until convergence decreased (SESS-$\partial(m)V$: from 7 for $\partial(2)$-V to 5 for $\partial(4)$-V; EE-$\partial(m)V$: from 8 for $\partial(2)$-V to 6 for $\partial(4)$-V).

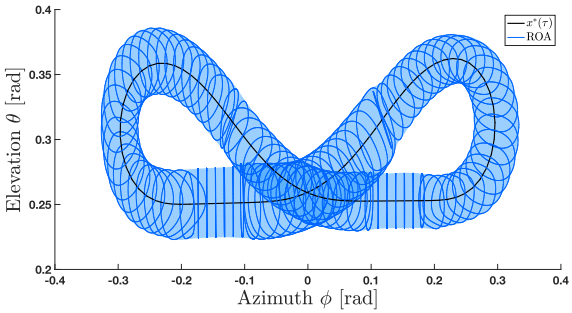

Fig. 3. The blue lines indicate the verified ROA on each hyperplane $S(\tau)$ obtained from EE-$\partial(4)V$.

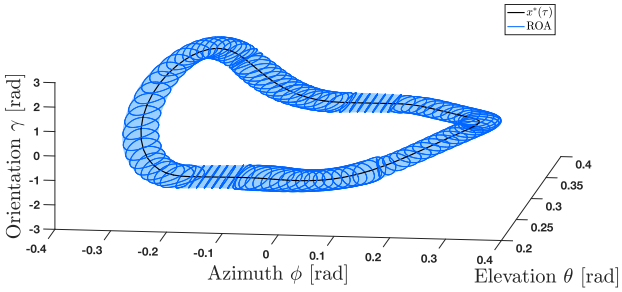

Fig. 4. A rotated 3D view of the ROA around the figure-of-eight trajectory obtained from EE-$\partial(4)V$, as displayed in Figure 3.

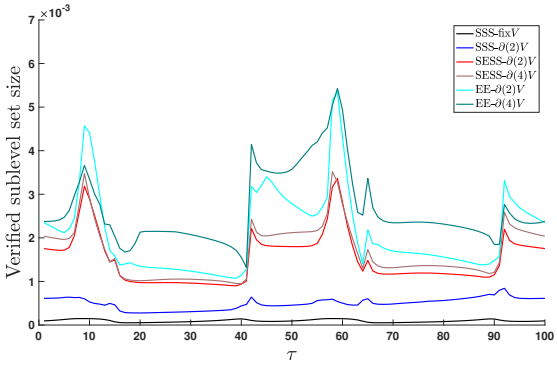

Fig. 5. The different lines indicate the sizes of verified ROA for the measure functions and degrees of V, as described in Subsection IV-B.

VI. Conclusion

In this work we generated feedback stabilized optimal trajectories for the path-following of power kites and verified the stabilizing region of the feedback gains by employing SOS-based relaxations of transverse stability conditions. We find that both the choice of the ROA measure function as well as the degree of the class of LFs can considerably change the verified ROA.

References

[1] M. Loyd, "Crosswind kite power (for large-scale wind power production)," *J. Energy*, vol. 4, no. 3, pp. 106–111, 1980.

[2] U. Ahrens, M. Diehl, and R. Schmehl, *Airborne Wind Energy*. Heidelberg, Germany: Springer, 2013.

[3] L. Fagiano, A. U. Zgraggen, M. Morari, and M. Khammash, "Automatic crosswind flight of tethered wings for airborne wind energy: modeling, control design and experimental results," *IEEE Trans. Control Syst. Technol.*, vol. 22, no. 4, pp. 1433–1447, 2014.

[4] M. Erhard and H. Strauch, "Flight control of tethered kites in autonomous pumping cycles for airborne wind energy," *Control Eng. Pract.*, vol. 40, pp. 13–26, 2015.

[5] N. Rontsis, S. Costello, I. Lymperopoulos, and C. N. Jones, "Improved path following for kites with input delay compensation," in *IEEE Conf. Decis. Control*. IEEE, 2015, pp. 656–663.

[6] T. A. Wood, H. Hesse, and R. S. Smith, "Predictive Control of Autonomous Kites in Tow Test Experiments," *IEEE Control Syst. Lett.*, vol. 1, no. 1, pp. 110–115, 2017.

[7] C. Jehle and R. Schmehl, "Applied Tracking Control for Kite Power Systems," *J. Guid. Control. Dyn.*, vol. 37, no. 4, pp. 1211–1222, 2014.

[8] T. A. Wood, H. Hesse, A. U. Zgraggen, and R. S. Smith, "Model-based flight path planning and tracking for tethered wings," in *Proc. IEEE Conf. Decis. Control*, 2015, pp. 6712–6717.

[9] R. Tedrake, I. R. Manchester, M. Tobenkin, and J. W. Roberts, "LQR-trees : Feedback Motion Planning via Sums-of-Squares Verification," *Int. J. Rob. Res.*, vol. 29, no. 8, pp. 1038–1052, 2010.

[10] M. M. Tobenkin, I. R. Manchester, and R. Tedrake, "Invariant Funnels around Trajectories using Sum-of-Squares Programming," in *IFAC Proc. Vol.*, vol. 44, no. 1. IFAC, 2011, pp. 9218–9223.

[11] I. R. Manchester, "Transverse Dynamics and Regions of Stability for Nonlinear Hybrid Limit Cycles," in *IFAC Proc. Vol.*, vol. 44, no. 1. IFAC, 2011, pp. 6285–6290.

[12] I. R. Manchester, M. M. Tobenkin, M. Levashov, and R. Tedrake, *Regions of Attraction for Hybrid Limit Cycles of Walking Robots*. IFAC, 2011, vol. 44, no. 1.

[13] J. Z. Tang, A. M. Boudali, and I. R. Manchester, "Invariant funnels for underactuated dynamic walking robots: New phase variable and experimental validation," in *2017 IEEE Int. Conf. Robot. Autom.* IEEE, 2017, pp. 3497–3504.

[14] P. A. Parrilo, "Structured Semidefinite Programs and Semialgebraic Geometry Methods in Robustness and Optimization," Ph.D. dissertation, California Institute of Technology, 2000.

[15] Z. Jarvis-Wloszek, R. Feeley, W. Tan, K. Sun, and A. Packard, "Controls Applications of Sum of Squares Programming," in *Posit. Polynomials Control*. Springer, Berlin, Heidelberg, 2005, pp. 3–22.

[16] W. Tan and A. Packard, "Stability Region Analysis Using Polynomial and Composite Polynomial Lyapunov Functions and Sum-of-Squares Programming," *IEEE Trans. Automat. Contr.*, vol. 53, no. 2, pp. 565–571, 2008.

[17] M. A. Patterson and A. V. Rao, "GPOPS-II: A MATLAB Software for Solving Multiple-Phase Optimal Control Problems Using hp-Adaptive Gaussian Quadrature Collocation Methods and Sparse Nonlinear Programming," *ACM Trans. Math. Softw.*, vol. 41, no. 1, pp. 1–37, 2014.

[18] P. Giesl, "On the determination of the basin of attraction of periodic orbits in three- and higher-dimensional systems," *J. Math. Anal. Appl.*, vol. 354, no. 2, pp. 606–618, 2009.

[19] J. Hauser and C. C. Chung, "Converse Lyapunov functions for exponentially stable periodic orbits," *Syst. Control Lett.*, vol. 23, pp. 27–34, 1994.

[20] H. Khalil, *Nonlinear Systems*, 3rd ed. Prentice Hall, Upper Saddle River, 2002.

[21] J. K. Hale, *Ordinary Differential Equations*. R.E. Krierger Pub. Co., New York, 1980.

[22] G. Stengle, "A Nullstellensatz and a Positivstellensatz in Semialgebraic Geometry," *Math. Ann*, vol. 207, pp. 87–97, 1974.

[23] A. Majumdar, A. A. Ahmadi, and R. Tedrake, "Control Design along Trajectories with Sums of Squares Programming," in *2013 IEEE Int. Conf. Robot. Autom.* IEEE, 2013, pp. 4054–4061.

[24] S. Bittanti, P. Colaneri, and G. D. Nicolao, "The Periodic Riccati Equation," in *Riccati Equ.*, S. Bittanti, A. Laub, and J. Williams, Eds. Springer, Berlin, 1991, pp. 127–162.

[25] J. Lofberg, "Pre- and Post-Processing Sum-of-Squares Programs in Practice," *IEEE Trans. Automat. Contr.*, vol. 54, no. 5, pp. 1007–1011, 2009.